PHYSICAL REVIEW E **74**, 030702(R) (2006)

Smectic-C^*_α–smectic-C^* phase transition and critical point in binary mixtures

Z. Q. Liu,[1] S. T. Wang,[1,*] B. K. McCoy,[1] A. Cady,[1,†] R. Pindak,[2] W. Caliebe,[2,‡] K. Takekoshi,[3] K. Ema,[3] H. T. Nguyen,[4] and C. C. Huang[1]

[1]*School of Physics and Astronomy, University of Minnesota, Minneapolis, Minnesota 55455, USA*

[2]*NSLS, Brookhaven National Laboratory, Upton, New York 11973, USA*

[3]*Department of Physics, Graduate School of Science and Engineering, Tokyo Institute of Technology, 2-12-1 Oh-okayama, Meguro, Tokyo, 152-8550, Japan*

[4]*Centre de Recherche Paul Pascal, CNRS, Université Bordeaux I, Avenue A. Schweitzer, F-33600 Pessac, France*

(Received 16 April 2006; published 26 September 2006)

We have investigated the smectic-C^*_α–smectic-C^* (SmC^*_α-SmC^*) transition in a series of binary mixtures with resonant x-ray diffraction, differential optical reflectivity, and heat capacity measurements. Results show that the phases are separated by a first-order transition that ends at a critical point. We report the observation of such a critical point. We have proposed the appropriate order parameter and obtained values of two critical exponents associated with this transition. The values of the critical exponents suggest that long-range interactions are present in the SmC^*_α-SmC^* critical region.

DOI: 10.1103/PhysRevE.74.030702 PACS number(s): 64.70.Md, 61.30.Gd

Liquid crystals are phases with intermediate order between solids and liquids. The intermediate ordering of liquid crystals gives rise to rich structures and transitions of great value to both science and technology. Smectic liquid crystals exhibit layered structures and manifest various in-layer orientational orders in different phases. Chiral rodlike smectigens form layered phases in which molecules tilt uniformly in each layer, while tilt orientations change from layer to layer [1–3]. The smetic-C^* (SmC^*) phase has a helical pitch (ξ) associated with the tilt orientation, usually several hundred nanometers long. The SmC^*_α phase, which exists at a higher temperature than the SmC^* phase, manifests a shorter pitch in the range of nanometers. Many compounds show both phases below T_{AC} (SmA-SmC^*_α transition temperature). The pitch evolves with temperature between the phases. The evolution can either be continuous or show a discrete jump [4,5], which has a very subtle dependence on the compound. Even some consecutive members of homologous compounds display completely different pitch evolutions [4]. Since there is no symmetry breaking through the SmC^*_α-SmC^* transition, a critical point must exist in the phase diagram. This phase transition, although in a totally different physical situation, resembles the liquid-gas phase transition in many aspects. In order to gain more physical intuition, we relate thermodynamic parameters in this smectic system (temperature, helical pitch, and mixture concentration) with corresponding parameters in the liquid-gas system (temperature, density, and pressure). The helical pitch behaves similarly to the density, as they are both discontinuous across the phase boundary and continuous beyond a critical point. In order to prove this prediction, a detailed study of an appropriate system is needed. Through the study of the critical exponents of such a system, we can also shed some light on a long-standing question: are there any long-range interactions in the smectic liquid crystals or not? Our detailed studies of two groups of binary mixtures from a unique homologous series allowed us to acquire critical physical properties of the smectic system near the critical point, namely, the identification of the relevant order parameter and determination of two critical exponents. Our results proved the existence of a critical point and suggested long-range interactions in the smectic system.

In this Rapid Communication we present resonant x-ray diffraction (RXRD) and heat capacity measurements on the mixture system. Various binary mixtures were made from three homologs, 10-, 11-, and 12-OTBBB1M7 (C10, C11, and C12). The Cn homologs all have one sulfur atom in their core parts, which enables us to use RXRD to directly study the pitch evolution with high resolution. Their chemical structures are shown at the top of Fig. 1. C10 exhibits decrease of pitch upon cooling [6]. C11 shows increase of pitch with decreasing temperature and makes a small jump into a longer pitch at the transition [5]. C12 shows a continuous evolution of the pitch, increasing upon cooling. Mixing C10 with C11 will provide us critical insight into the first-order transition, while mixing C11 with C12 should provide us physical properties of either the first-order transition or continuous evolution, depending on the ratio of C11 and C12. We will use a letter C followed by a concentration number n to refer to the different pure and mixed samples. Each sample is associated with a number between 10.00 and 12.00. For instance, the 20% C10–80% C11 (96% C11–4% C12) mixture is referred to as C10.80 (C11.04). Within our resolution this notation allows us to describe the changes in physical parameters from C10-C11 to C11-C12 mixtures smoothly. n serves as a thermodynamic parameter in our fitting.

RXRD has become a powerful probe to directly study nanoscale molecular orientations in liquid crystal systems since it was introduced [8]. The samples need to be specially prepared to contain heavy elements in their core parts, sulfur

*Present address: NSLS, Brookhaven National Laboratory, Upton, New York 11973.

†Present address: Advanced Photon Source, Argonne National Laboratory, Argonne, Illinois 60439.

‡Present address: HASYLAB at DESY, Notkestrasse 85, D-22603 Hamburg, Germany.

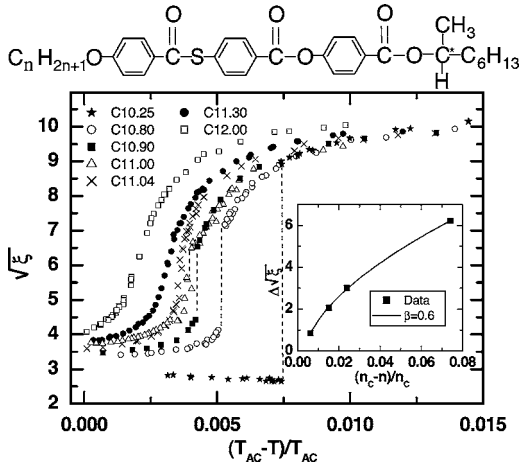

FIG. 1. Pitch evolution of pure compounds and mixtures of C*n*. The temperatures are normalized to T_{AC}. The dashed lines are used to mark jumps of pitch across the phase boundary. The magnitudes of $\Delta\sqrt{\xi}$ were used to extrapolate the critical concentration $n=11.07$. The inset is the fitting of the critical exponent β. The molecular structure of the C*n* molecules is shown at the top. The phase sequence of C10 is in [7].

in our case. The incident x-ray energy is tuned to the fluorescent peak obtained from K_α absorption of the heavy element. Since the heavy element is bonded to the molecular core part, its bonding orientation with respect to the incident x-ray changes as the orientations of the molecules change from layer to layer. Periodic orientational modulations of the molecules from layer to layer result in interference of the x-rays emitted from the heavy elements in different layers. Thus the orientational periodicity creates satellite peaks that appear around the main diffraction peaks from the smectic layers. The distance from the satellites to their corresponding main peaks gives the periodicity of the molecular tilt direction, i.e., pitch, in the SmC^*_α or SmC^* phase. Our RXRD experiments were conducted at beamline X19A at the NSLS, Brookhaven National Laboratory. Samples were loaded in a temperature-controlled two-stage oven sealed and flushed with He to reduce sample degradation and air absorption of the x-rays. The oven was mounted on a two-circle Huber diffractometer. The detailed experimental setup was described elsewhere [6]. Thick free-standing films were pulled with a glass spreader across a rectangular hole on a stainless steel film plate. The x-ray diffraction geometry is simple since the layers are parallel to the film surface. Powder samples were used to determine the optimal resonant energy prior to diffraction experiments. The x-ray energy was then fixed at the fluorescence peak throughout the experiment. The first- and second-order main diffraction peaks were acquired with the satellite peaks for accuracy. Usually the temperature was increased from the SmC^* phase to the SmC^*_α phase in small steps and several iterations were performed. A second film was usually studied to confirm data reproducibility.

Prior to RXRD studies, the mixtures were characterized with our in-house differential optical reflectivity studies [9]. The temperature ranges of relevant phases and behaviors were acquired and several mixtures were selected for detailed studies with RXRD.

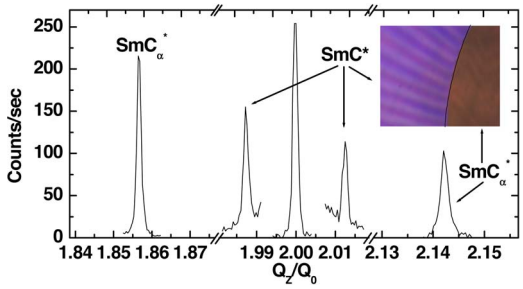

FIG. 2. (Color online) Coexistence of the SmC^*_α and SmC^* phases at 120.0 °C in the C10.25 mixture. Two sets of satellite peaks were found, representing the SmC^*_α and SmC^* phases. The locations of the peaks are 1.856, 1.987, 2.000, 2.012, and 2.142. The pitch is 81.0 layers (SmC^*) and 7.00 layers (SmC^*_α). The inset shows a picture of the coexistence with a clear phase boundary in the middle. The black curve is an aid to the eye. The left side is in the SmC^* phase; the film appears purple. The right side is in the SmC^*_α phase; the pitch is too short to reflect visible light. The brown color comes from reflection of a copper plate underneath the film.

We will separately discuss our findings in two series of mixtures, those from mixtures of C10 with C11 (C10.*xx*), and those from mixtures of C11 with C12 (C11.*xx*). C10.*xx* mixtures that we studied all showed discrete jumps of the pitch at $T_C(n)$ (the SmC^*_α-SmC^* transition temperature in the sample C*n*). The main features found in the SmC^*_α phase are the following. The C10.25 mixture showed a constant positive $d\xi/dT$. The pitch just below T_{AC}, from linear extrapolation, is about 8.6 layers, which decreases upon cooling. The pitch was 7.0 layers just above $T_C(10.25)$. The C10.80 and C10.90 mixtures both showed a negative $d\xi/dT$. The pitch is about 10 layers below T_{AC}, increasing slightly upon cooling. $d\xi/dT$ turns from positive to negative as n increases from 10.25 to 10.80. In the SmC^* phase, $|d\xi/dT|$ decreases toward lower temperature. We plotted the pitch evolutions of the mixtures in Fig. 1. The reason we used $\sqrt{\xi}$ instead of ξ as the vertical axis will be explained in the discussion of critical exponents. The vertical dashed lines are aids to the eye for jumps of the pitch across the transition. These curves resemble the isobars of a liquid-gas system. $\Delta\sqrt{\xi}$ is the magnitude of the jump in $\sqrt{\xi}$ at $T_C(n)$. $\Delta\sqrt{\xi}$ with different concentrations were extrapolated to obtain the critical concentration $n_C=11.07$. Furthermore, in the C10.25 mixture, we observed coexistence of the SmC^*_α and SmC^* phases at the transition. Figure 2 shows scans around the second-order ($L=2$) main diffraction peak from C10.25. Scans revealed four satellite peaks. The two peaks that are closer to $L=2$ signified a pitch of 81.0 layers; the other two yielded a pitch of 7.00 layers. The temperature stability during the scans was slightly better than 0.01 °C. The coexistence has a window of about 0.1 °C. Within the coexistence temperature window, a clear phase boundary was observed and photographed (Fig. 2 inset). Above and below the coexistence, the film appeared to be uniform and only one set of resonant peaks was detected. Similar behavior was also observed in the other C10.*xx* mixtures. This observation indicates a first-order transition.

The C11.*xx* mixtures that we studied (C11.04–C11.50) all showed continuous evolution of the pitch upon cooling.

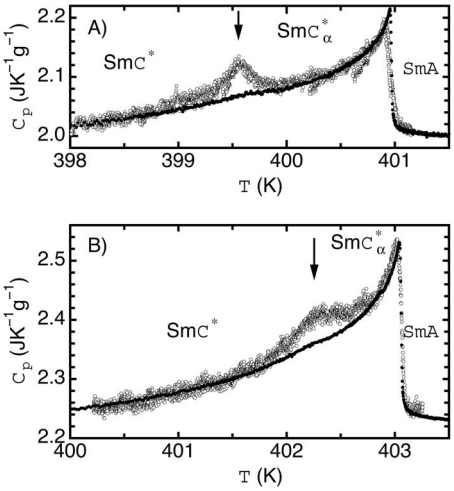

FIG. 3. Heat capacity measurements of C11.04 (a) and C12 (b). In NAS mode (open circles), both samples showed an anomaly around the transition temperature. The anomaly is more pronounced than in the ac mode (solid dots). From NAS results, the C11.04 mixture shows almost critical behavior at the SmC^*_α-SmC^* phase transition. The C12 shows supercritical behavior in the shape of a wide hump.

We studied in detail C11.04, C11.30, and C12.00. The maximum value of $|d\xi/dT|$ increases as n decreases from 12.00 to 11.04, and reaches a very large value for C11.04. This evolution indicates that the system approaches the critical point. Within our resolution, the C11.04 mixture showed a continuous evolution. According to our fitting from the C10.xx mixtures (Fig. 1 inset), C11.04 should have a pitch jump of about five layers. This amount of pitch change corresponds to about 0.005 °C temperature change, less than the temperature stability of our system. Within our resolution, the C11.04 mixture is very close to the critical mixture.

To determine the nature of the SmC^*_α-SmC^* transition, the heat capacity has also been measured using a high-resolution calorimeter. The calorimeter can be operated in a low-frequency ac mode as well as in a nonadiabatic scanning (NAS) mode [10,11]. The samples were placed in hermetically sealed gold cells. The temperature scan rate was about 0.14 K/h in the transition region. In addition to our previous results from pure C11 [12], two more samples, pure C12 and C11.04, were studied. In the ac mode, the measured heat capacity (C_P) data (Fig. 3) show extremely small changes near the SmC^*_α-SmC^* transition, while in the NAS mode, the acquired data exhibit anomalous behavior. The data are reproducible between four (for C12) or three (for C11.04) pairs of heating and cooling runs, except that the overall $C_P(T)$ behavior showed a slow temperature drift with a rate of less than 50 mK/day. There is no observable thermal hysteresis in C12 or C11.04. In contrast to the data from pure C12, a sharper and more symmetric C_P peak was obtained from the C11.04 mixture. This result strongly supports the conclusion from our RXRD data that the C11.04 sample is very close to the critical mixture associated with the SmC^*_α-SmC^* transition. We also note that the failure of the ac-mode measurement in detecting the C_P anomaly indicates that a quite sluggish relaxation process accompanies the transition, so that the ac power input at 0.032 Hz was too fast for the system to follow.

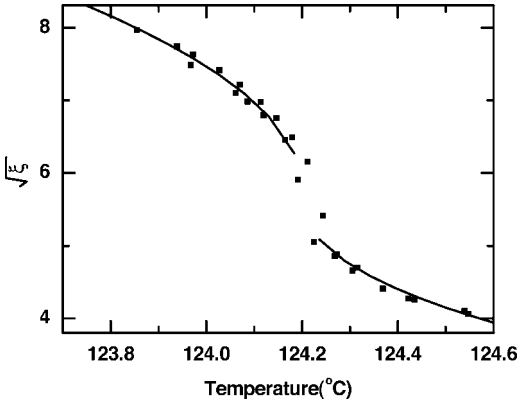

FIG. 4. Temperature evolution of $\sqrt{\xi}$ for the C11.04 mixture. Solid lines are fitting results using Eq. (1).

With results mentioned above, we show that the transition is clearly first order and has a critical point. In order to gain more insight into the system, we need to further determine the order parameter and extract the revelent critical exponents. The liquid-gas system and binary fluid system, which are similar to this smectic system, with no symmetry breaking across the transition, are described by the basic critical exponents α, β, γ, and δ. From our data, we were able to extract β and δ. In the liquid-gas system, the critical isobar is associated with the critical exponent δ. Correspondingly, in the smectic system, the critical isochore (C11.04) is related to δ with the same relation:

$$d - d_C = A^{\pm}|T - T_C(n)|^{1/\delta}. \quad (1)$$

Here d is the order parameter; d_C is the value of the order parameter at the critical point. $A^{\pm}$ is the magnitude just above and below $T_C(n)$. The quantities ξ, $2\pi/\xi$ (azimuth change between adjacent layers), and $\sqrt{\xi}$ have been considered as the order parameters. Fitting results showed that assuming $\sqrt{\xi}$ as the order parameter makes the isochore most symmetric around T_C, producing the best fit. The fitting yields $d_C = 5.8 \pm 0.2$, $|A^+/A^-| = 0.4 \pm 0.1$, $\delta = 2.3 \pm 0.4$, $T_C = 124.20 \pm 0.03$ °C. δ from a mean-field calculation is 3. Fitting results are shown in Fig. 4.

In the vicinity of the critical point on the coexistence curve, to a good approximation, n is proportional to T. As a result, β can be obtained from fitting the order parameter with n ($\Delta d = B|n - n_C|^{\beta}$). Each mixture's temperature data have been shifted slightly to account for thermal degradation and x-ray damage. The shift, although small compared to $T_C(n)$, introduced a large relative uncertainty among the $T_C(n)$ in different mixtures. On the other hand, the accuracy of concentration is much higher. Thus we decided to extract β from n. We found that assuming $\Delta\sqrt{\xi}$ as the order parameter, β is 0.6 ± 0.1, close to the mean-field prediction of 1/2. $\Delta\sqrt{\xi}$ vs $(n_C - n)/n_C$ was plotted in the inset of Fig. 1. It is worth mentioning that during the temperature evolution of the helical pitch, the molecular tilt also changed by about 3% within the temperature window. The change was very

smooth and was very unlikely to be a dominant factor of the transition.

To summarize, we have conducted extensive studies of the SmC^*_α-SmC^* phase transition on pure Cn compounds and their binary mixtures. We conclude that the SmC^*_α-SmC^* phase transition is a first-order phase transition, which ends at a critical point. The critical point is at $n_C=11.07$, $T_C=124.2$ °C, $\sqrt{\xi_C}=6$. We found that the transition is characterized by an order parameter $\sqrt{\xi}$. The critical exponent δ is about 2.5, and β is about 1/2, close to mean-field values. Previous results suggest that the short pitch in the SmC^*_α phase results from competition between short-range interactions [4,14] (nearest-neighbor-layer ferroelectriclike coupling and next-nearest-neighbor-layer antiferroelectriclike coupling). The mean-field-like critical exponents suggest that long-range interactions also play a role. One group has derived an effective long-range interaction due to layer fluctuation [13]. Their model produces all known SmC^* variant phases. Whether this type of long-range interaction is responsible for the observed SmC^*_α-SmC^* critical behavior remains to be investigated.

We are grateful to Professor P. Barois for lending us his x-ray oven during our entire studies. We would also like to thank L. Glazman, M. Garst, and Y. Lu for valuable discussions. Research at the NSLS, BNL was supported in part by the U.S. Department of Energy, Division of Materials Sciences and Division of Chemical Sciences, under Contract No. DE-AC02-98CH10886. The research was supported in part by the donors of the Petroleum Research Fund, administered by the American Chemistry Society and by the National Science Foundation, Solid State Chemistry Program under Grant No. DMR-0106122. Z.Q.L. and B.K.M acknowledge support from the University of Minnesota Graduate School.

[1] M. Fukui, H. Orihara, Y. Yamada, N. Yamamoto, and Y. Ishibashi, Jpn. J. Appl. Phys., Part 2 **28**, L849 (1989).

[2] R. B. Meyer, L. Liebert, I. Strzelecki, and P. Keller, J. Phys. (Paris), Lett. **36**, L69 (1975).

[3] A. Fukuda, Y. Takanishi, T. Isozaki, K. Ishikawa, and H. Takezoe, J. Mater. Chem. **4**, 997 (1994).

[4] A. Cady, D. A. Olson, X. F. Han, H. T. Nguyen, and C. C. Huang, Phys. Rev. E **65**, 030701(R) (2002).

[5] C. C. Huang, Z. Q. Liu, A. Cady, R. Pindak, W. Caliebe, P. Barois, H. T. Nguyen, K. Ema, K. Takekoshi, and H. Yao, Liq. Cryst. **31**, 127 (2004).

[6] P. Mach, R. Pindak, A.-M. Levelut, P. Barois, H. T. Nguyen, H. Baltes, M. Hird, K. Toyne, A. Seed, J. W. Goodby, C. C. Huang, and L. Furenlid, Phys. Rev. E **60**, 6793 (1999).

[7] The phase sequence for C10 is Iso(153 °C)SmA(124 °C)SmC^*_α(119 °C)SmC^*_{FI2}(114 °C)SmC^*_{FI1}(112 °C)SmC^*_A.

[8] P. Mach, R. Pindak, A.-M. Levelut, P. Barois, H. T. Nguyen, C. C. Huang, and L. Furenlid, Phys. Rev. Lett. **81**, 1015 (1998).

[9] S. Pankratz, P. M. Johnson, and C. C. Huang, Rev. Sci. Instrum. **71**, 3184 (2000).

[10] K. Ema and H. Yao, Thermochim. Acta **304/305**, 157 (1997).

[11] H. Yao, K. Ema, and C. W. Garland, Rev. Sci. Instrum. **69**, 172 (1998).

[12] The heat capacity data from pure C11 were reported in Ref. [5]. Thermal hysteresis between cooling and heating runs was observed.

[13] M. B. Hamaneh and P. L. Taylor, Phys. Rev. Lett. **93**, 167801 (2004).Phys. Rev. E **72**, 021706 (2005).

[14] V. P. Panov, B. K. McCoy, Z. Q. Liu, J. K. Vij, J. W. Goodby, and C. C. Huang, Phys. Rev. E **74**, 011701 (2006).